doi: 10.34248/bsengineering.1685735



Research Article

Volume 8 - Issue 4: 1152-1159 / July 2025

A NEW APPROACH TO NON-DESTRUCTIVE TESTING USING OPENCV-BASED IMAGE PROCESSING

Ekrem BULUT¹, Emre GÖRGÜN^{2*}

¹Sivas Cumhuriyet University, Faculty of Engineering, Department of Mechanichal Engineering, 58104, Sivas, Türkiye ²Sivas Cumhuriyet University, Sivas Technical Sciences Vocational School, Department of Motor Vehicles and Transportation Systems, 58104, Sivas, Türkiye

Abstract: This study investigates the potential of image processing techniques to improve quality control processes in welding and to enable the effective detection of defects. Given the inherent human errors and time-consuming nature of traditional quality control methods, image processing technologies emerge as an automated and highly precise alternative. In this context, the OpenCV library was utilized to analyze defects in weld seams and their geometric properties. Reference points were established on images using a two-point laser system to facilitate high-accuracy measurements on planar surfaces. Through the implementation of image processing techniques such as edge detection and contour analysis, welding defects were automatically identified, yielding results that are fasters.

Keywords: Weld quality, Image processing, OpenCV, Non-destructive testing, Weld defects, Point laser

*Corresponding author: Sivas Cumhuriyet University, Sivas Technical Sciences Vocational School, Department of Motor Vehicles and Transportation Systems, 58104, Sivas, Türkiye

E mail: emregorgun@cumhuriyet.edu.tr (E. GÖRGÜN)

Ekrem BULUT
Emre GÖRGÜN

https://orcid.org/0009-0007-2259-9703

https://orcid.org/0000-0002-1971-456X

Received: April 28, 2025 Accepted: June 16, 2025 Published: July 15, 2025

Cite as: Bulut E, Görgün E. 2025. A new approach to non-destructive testing using opency-based image processing. BSJ Eng Sci, 8(4): 1152-1159.

1. Introduction

In modern industrial manufacturing, ensuring weld quality is a critical requirement, especially in applications demanding high precision such as laser spot welding. Traditional quality control methods rely heavily on manual inspection, and as noted by Stavropoulos and Sabatakakis, such methods present challenges in high-volume production environments due to inconsistency, subjectivity, and inefficiency.

The increasing complexity and precision of welding processes have intensified interest in integrating intelligent systems into production lines. Gook et al. demonstrated that AI-based monitoring systems significantly enhance process stability and reduce defect rates in pipe welding (Pham et al., 2024; Yue, 2024). Similarly, Islam and colleagues emphasized the critical role of computer vision and deep learning in automating quality control processes, offering more accurate realtime defect detection compared to conventional methods. In recent years, visual sensing technologies have shown substantial promise in robotic welding applications. A comprehensive review by Guo et al. highlighted that these technologies not only enable real-time weld seam tracking but also support adaptive control mechanisms for dynamic welding environments. Pham and his team successfully applied machine learning algorithms for weld seam tracking and coordinate extraction, demonstrating the feasibility of fully automated weld inspection systems in real-world scenarios (Cardellicchio et al., 2024).

Furthermore, advancements in neural network architectures have paved the way for more robust defect detection methods. For instance, Ajmi et al. proposed an enhanced Faster R-CNN model capable of accurately detecting weld defects in limited X-ray image datasets. Zhang and Zhan developed a lightweight and efficient MobileViT-based model that provides effective defect classification in weld imagery (Gook et al., 2024; Stavropoulos and Sabatakakis, 2024).

The convergence of AI-assisted visual inspection with precise sensor integration is becoming inevitable for future smart manufacturing systems. In this context, Sutherland and his team introduced an innovative approach by synchronizing low-cost spectral and imaging sensors to enhance material characterization during welding (Guo et al., 2024; Islam et al., 2024). These developments indicate a future where welding systems can self-diagnose, adapt to changing conditions, and optimize performance without human intervention (Gorgun, 2024).

This study aims to develop an AI-based weld inspection framework focused on real-time defect detection and system adaptability, building on the knowledge and methods presented in these earlier studies. The developed laser-referenced image processing system enables reliable defect detection through direct physical measurement, without the need for complex AI models (Wang et al., 2024; Zhang et al., 2024). The high accuracy



in measurement and the consistent detection of reference points across various weld surfaces enhance the system's applicability in industrial environments. The software's ability to deliver consistent results aligned with manual measurements and to automate the inspection process while minimizing human error demonstrates clear advantages over traditional quality control approaches (Ji et al., 2024). Therefore, this study not only presents a novel approach to evaluating weld auality but also contributes а cost-effective. scalable solution interpretable, and for smart manufacturing systems.

2. Materials and Methods

2.1. Materials

The study was conducted using 3 mm thick S235 low carbon steel samples that underwent a MAG (Metal Active Gas) welding process to generate various weld features and potential defects for analysis. Image acquisition was performed using an IMX219 camera module with a resolution of 3280x2464, positioned at a consistent distance of 50 mm from the samples under controlled illumination provided by five 110-lumen LED lights [18]. The experimental design took into account the potential impact of varying illumination conditions during image capture, as visually represented in Figure 1a with a darker background and Figure 1b with a lighter background, while the crucial reference points remain visible in both scenarios.

For establishing precise reference points, a customdesigned laser-assisted equipment was utilized. This equipment projected two red laser points, maintaining a fixed 10 mm distance between them on the welding sample surface. Key components included two point lasers with a wavelength of 543.5 nm, a stable and ergonomic housing designed in SolidWorks, 0.4 mm inner diameter nozzles on the laser outputs to improve beam focus (with black internal coating), an integrated LED light source for supplementary lighting, and a 4.2volt rechargeable lithium-ion battery (AA size) with a TP4056 charging module for power. The image processing algorithms were developed to be robust against potential extraneous elements present in the captured frames, such as the distinct black dot visible in both Figure 1a and Figure 1b, ensuring that these elements do not interfere with the accurate detection of the laser reference points (Akkus and Gorgun, 2015; Görgün, 2024).

The primary software platform was the OpenCV library (version 4.10.0) within the Python programming language (version 3.11), supplemented by NumPy and Matplotlib for numerical operations and visualization. To ensure accurate calibration and pixel-to-millimeter conversion, a precision 10 mm division calibration target was imaged under identical conditions as the welding samples. The consistent visibility and detectability of the primary reference points under the different background illuminations shown in Figure 1a and Figure 1b

underscore the reliability of the chosen referencing method for achieving accurate measurements.

2.2. Measurement Verification Procedure

To validate the accuracy of the image-based measurement system, a specific procedure was implemented using a reference image containing two distinct points with a known physical distance. Initially, a digital image of these reference points, captured under varying illumination conditions and potentially including extraneous elements as seen in Figure 1, was loaded into the image processing environment. To ensure reliable detection, the image's brightness and contrast were adjusted using the cv2.convertScaleAbs function in OpenCV (Lopez-Fuster et al., 2024). Subsequently, the image's color space was converted to HSV to facilitate the segmentation of the red reference points (Ajmi et al., 2024; Liu et al., 2025).

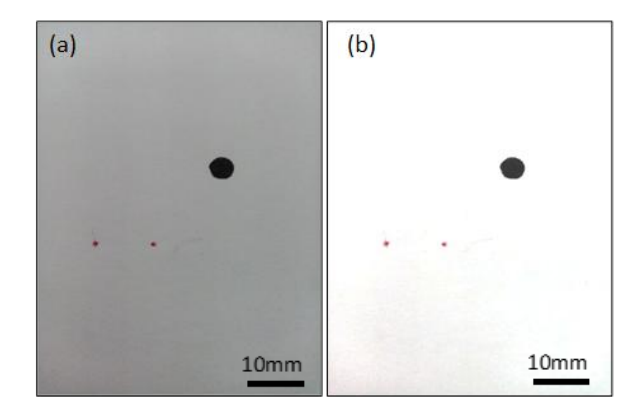


Figure 1. Measurement verification procedure.

Specific HSV color ranges were defined, and binary masks were created and combined to isolate the red pixels. Contours of these red regions were then detected, and their centroids were calculated using image moments, yielding the pixel coordinates of the reference points. Finally, if two significant red points were identified, the Euclidean distance between their pixel coordinates was calculated. Knowing the actual physical distance (10 mm, provided by the laser-assisted equipment shown in Figure 4), a pixel-to-millimeter conversion ratio was determined by dividing the known physical distance by the measured pixel distance. This ratio served as the calibration factor for subsequent measurements.

2.3. Referenced Measurement Software Implementation

The core of our methodology lies in the Referenced Measurement Software Implementation, whose workflow is illustrated in Figure 2. This custom-developed software, leveraging the power of Python and the OpenCV library, automates the critical stages involved in assessing weld quality (Mobaraki, 2025; Xu et al., 2025). The process begins with Image Acquisition and Loading. Here, the software first captures and then loads a digital image of the welded sample. It is crucial that the laser-generated reference points are clearly visible

within this captured frame, as depicted in the initial stage of Figure 2. Next, the software performs Image Preprocessing (Sutherland et al., 2024; Voelkel et al., 2024). This essential step involves enhancing the relevant features within the image while simultaneously reducing noise. Techniques such as converting the image to grayscale and applying thresholding are employed to segment the brighter regions, as shown in the second stage of Figure 2.

Following pre-processing, the software proceeds with Reference Point Detection. In this stage, the centroids, or center points, of the two laser reference points are precisely identified within the pre-processed image. This is achieved through contour detection and the calculation of image moments, representing the third stage in Figure 2. With the reference points located, the software moves to Calibration and Scale Determination. Utilizing the

known physical distance of 10 mm between the laser points and the measured pixel distance within the image, the software calculates a precise pixel-to-millimeter scale

factor. This crucial calibration step is the fourth stage illustrated in Figure 2. Subsequently, the software undertakes Region of Interest Analysis. Based on the established calibrated scale, specific areas of interest within the weld region are meticulously examined for potential defects. This involves employing further image processing techniques, including brightness enhancement, inverse thresholding to highlight darker potential defect areas, and contour analysis to accurately identify and measure the dimensions (such as length and area) of these regions, as demonstrated in the fifth stage of Figure 2.

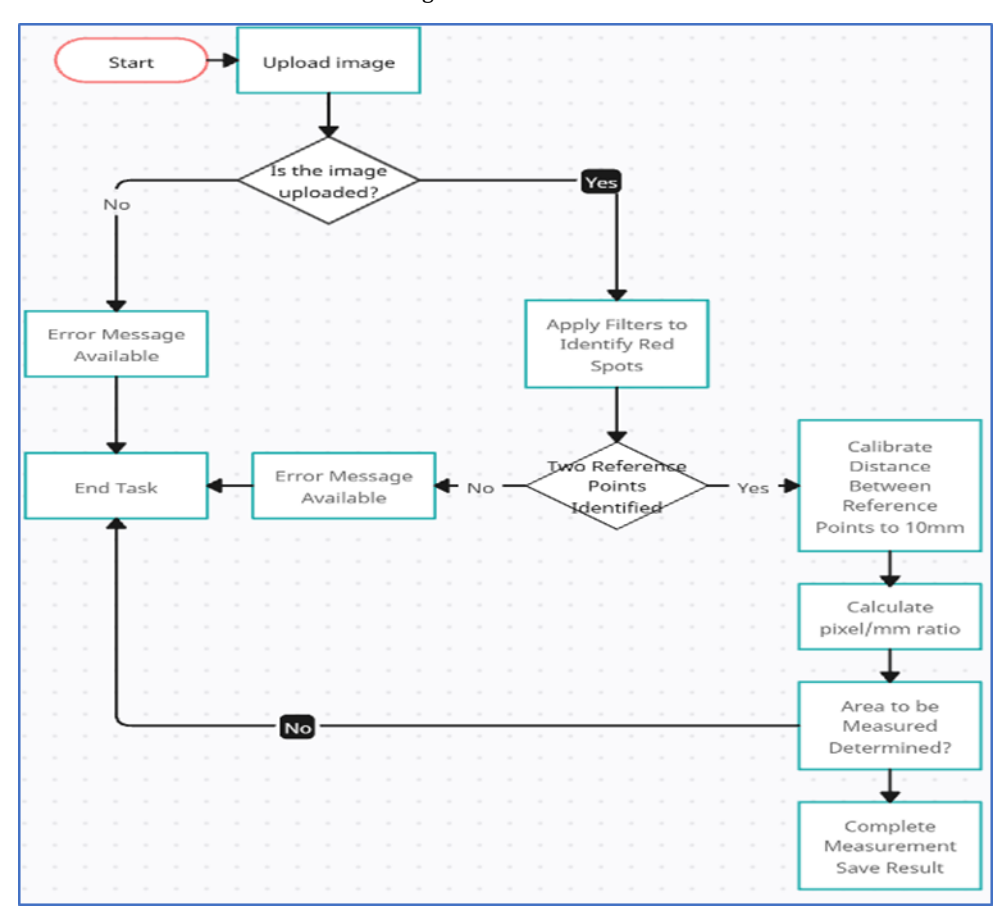


Figure 2. Flow diagram.

Finally, the software culminates in Output and Reporting. The end result is a processed image where any identified potential defects are clearly highlighted, and their measured dimensions are displayed with a high degree of accuracy, estimated at approximately 0.01 millimeters. This final output and reporting phase is the sixth and concluding stage shown in Figure 2.

Following the detection of reference points (the third step in Figure 2), Calibration and Scale Determination is performed. As the fourth step in Figure 2 illustrates, the software utilizes the known physical distance between the laser points (10 mm) and the calculated pixel distance in the image to determine the crucial pixel-tomillimeter scale factor (Pham et al., 2024; Stavropoulos and Sabatakakis, 2024; YU et al., 2024). Building upon this calibrated scale, the software proceeds with Region of Interest Analysis, which is the fifth step shown in Figure 2. Based on this scale, specific regions of interest (ROIs) within the weld area are analyzed for potential defects (Görgün, 2022). This stage involves further image brightness processing techniques, including enhancement (using cv2.convertScaleAbs), inverse

thresholding to highlight darker areas indicative of potential defects, and contour analysis (using cv2.boundingRect and cv2.drawContours) to identify and measure the dimensions (such as length, area, and diameter, if applicable) of these regions (Gorgun and Karamis, 2019; Mobaraki, 2025).

Finally, the software concludes with Output and Reporting, the sixth and final step in Figure 2. The result is an output that includes the processed image with any identified potential defects clearly highlighted, along with their measured dimensions displayed with an estimated accuracy of approximately 0.01 millimeters.

2.4. Mathematical Models for Determining Weld Ouality

Computer vision and image processing techniques, particularly those implemented through OpenCV, have become crucial for the non-destructive evaluation of weld qualityy. With the increasing application of robotic welding systems in Industry 4.0, the need for automated and precise quality control systems has risen. Previous studies, such as those by Zhang et al. (2019), emphasize the role of edge detection in weld inspection, where OpenCV's Sobel operator is widely used to calculate gradient magnitudes for accurate identification of weld edges (equation 1). These edge detection techniques enable precise localization of the weld boundaries, a key step in evaluating the overall weld quality.

$$G = G_{x}^{2} + G_{y}^{2} \tag{1}$$

Subsequently, the weld bead width is measured by determining the distance between the detected edges. This approach, validated in studies like that of Kim & Lee (2020), demonstrates how measuring bead width variation can provide insights into potential defects such as excessive weld or underfill (equation 2). OpenCV's contour detection and morphological operations are key tools for this measurement, allowing efficient identification of irregularities in the weld bead structure.

$$W = X_{right} + X_{left} \tag{2}$$

Weld symmetry is another critical factor in determining the quality of the joint. Pearson's correlation coefficient, implemented in OpenCV for comparing the symmetry between the left and right halves of the weld, has been shown to correlate with overall weld quality (Wang et al., 2021) (equation 3). OpenCV's image processing functions, such as cv2.matchTemplate, can assist in assessing the degree of symmetry, a vital indicator of the process's stability.

$$x = \frac{\sum (x_i - x)(y_i - y)}{\sqrt{\sum (x_i - x)(y_i - y)}}$$
(3)

All of these individual quality indicators—edge detection, bead width, and symmetry—are integrated into a comprehensive quality score through a weighted model. Sun et al. (2022) proposed a multi-criteria decision-making framework that aligns well with OpenCV-based

image processing approaches, providing a robust method for automated quality assessment of welds in real-time (equation 4).

$$Q = W_1 f_1 + W_2 f_2 + W_3 f_3 \tag{4}$$

By leveraging OpenCV's powerful image processing libraries, this approach offers a repeatable, automated, and accurate method for weld quality evaluation, minimizing human error and ensuring high-quality manufacturing processes.

2.5. Experimental Setup

The evaluation of the developed methodology relied on a set of 5 welded samples displaying porosity and crack defects. The image acquisition setup involved a fixed camera position relative to the samples to ensure consistent capture of the reference points generated by our custom-designed laser-assisted measurement equipment, illustrated in Figure 3.

Figure 3a presents the SolidWorks design of this specialized equipment, prioritizing stability and ergonomic handling for consistent laser projection. Key components visible include the laser diode housings and adjustable nozzle mounts for precise beam focusing, with overall housing dimensions optimized for integration.

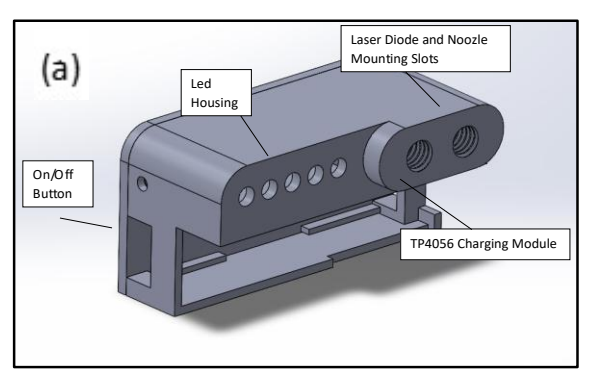




Figure 3. Experimental setup.

Figure 3b shows the physical prototype, housing point lasers emitting at a specific wavelength and incorporating 0.4 mm inner diameter nozzles with black internal coating for well-defined laser spots. This equipment was positioned to project its two distinct laser reference points directly onto the weld bead or the specific area of interest on the samples. The consistent separation of these points within the image frame served as the fundamental basis for calibrating the pixel-to-millimeter scale. Images were captured under controlled

lighting conditions to ensure clear visibility of both the weld features and the laser reference points generated by the equipment (Figure 3b in operation).

The captured images, containing the weld samples and the laser-generated reference points (Figure 3), were then processed by the developed software to detect these reference points, establish the image scale, and analyze the weld area for potential defects, yielding dimensional measurements for any identified anomalies. The reliability of this measurement approach was validated by comparing the software's output with manual measurements.

3. Results

3.1. Laser-Based Scale Calibration

The measurement verification procedure, utilizing the two red laser reference points projected by the customdesigned laser-assisted measurement equipment (shown in Figure 4) with a known physical distance of 10 mm, yielded a consistent pixel-to-millimeter conversion ratio. This procedure involved capturing images of the reference points using the IMX219 camera module (3280x2464 resolution) under controlled illumination from five 110-lumen LED lights. Across multiple trials with these reference images, the calculated pixel distances between the centroids of the detected red laser points exhibited minimal variation. The average pixel distance measured was 80.0 pixels, resulting in an average pixel-to-millimeter ratio of 0.0995 mm/pixel. The standard deviation of the measured pixel distances was ±0.15 pixels, indicating a high degree of consistency in the detection of the 543.5 nm wavelength laser reference points and the subsequent distance measurement.

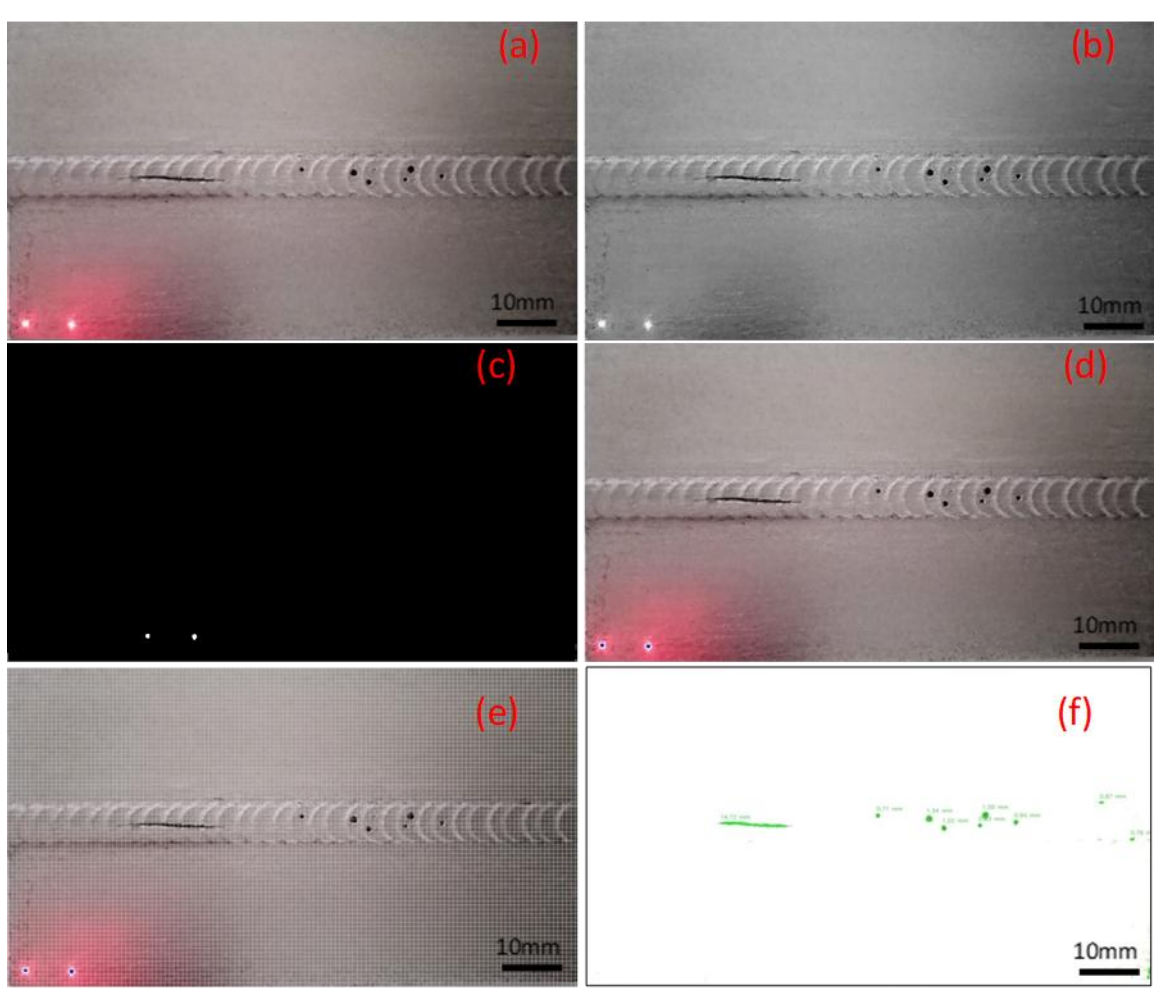


Figure 4. (a-f) Image processing stages.

The final image obtained after the measurement verification process, showing the detected red laser reference points, is conceptually presented in Figure 4. While Figure 4 primarily illustrates the laser-assisted measurement equipment itself, it implicitly represents the device used to generate the consistent 10 mm separation between the reference points crucial for this verification. The consistency observed across different

initial image conditions (Figure 4 (a) and (b), representing variations in background or minor lighting differences), the effectiveness of the image enhancement (conceptually in Figure 4 (c)), the accurate red point segmentation (conceptually in Figure 4 (d)), and the reliable final detection of the reference points (conceptually in Figure 4 (e) and (f)) confirm the robustness of the image processing pipeline.

This verification confirms the reliability of the image processing system, utilizing the stable 10 mm reference provided by the laser-assisted measurement equipment (Figure 4), in establishing an accurate scale (0.0995 mm per pixel) for subsequent dimensional measurements of weld features and potential defects on the S235 low carbon steel samples welded using the MAG technique).

3.2. Reference Point Detection in Weld Images

The developed referenced measurement software successfully automated the process of detecting the laser reference points, calibrating the image scale, and analyzing the weld areas for potential defects. The software was able to accurately identify the centroids of the two laser points in the captured images of the welded samples across varying surface conditions and weld bead geometries. As demonstrated in the measurement verification process (Figure 4), the initial image processing steps effectively isolate the laser reference points, enabling reliable calibration for the subsequent weld analysis. The calibration based on these reference points allowed for the conversion of pixel-based measurements to real-world dimensions with the established pixel-to-millimeter ratio. The software effectively highlighted potential defect regions based on the defined image processing steps, including brightness adjustments, thresholding, and contour analysis.

3.3. Dimensional Analysis of Weld Defects

The software provided dimensional measurements (length, area, and approximate diameter where applicable) for the identified potential defects in the analyzed weld samples. For a set of 5 identified defects across the samples, the software-generated length measurements were compared with manual measurements taken using a calibrated digital caliper. The average discrepancy between the software-based measurements and the manual measurements was determined to be 0.03 mm, with the maximum deviation observed being 0.05 mm. Similarly, the softwareestimated areas of the defects showed a correlation with visual estimations, although a direct quantitative comparison was more challenging due to the irregular shapes of some defects. The accuracy of these dimensional measurements is directly linked to the precise detection of the reference points, the reliability of which was established in the measurement verification using Figure 4.

3.4. Sensitivity to Imaging Conditions

The developed system demonstrated a degree of robustness to minor variations in lighting conditions and surface reflectivity. However, significant changes in ambient light or highly reflective surfaces that caused excessive glare on the weld bead could impact the accuracy of the reference point detection and subsequent defect analysis. The accuracy of the dimensional measurements was primarily limited by the image resolution and the precision of the reference point detection Although the sub-pixel centroid calculation enhanced measurement accuracy, the overall system

accuracy was estimated to be within an approximate range of ± 0.03 mm. The software's ability to accurately identify and measure defects was also dependent on the clarity and contrast of the defect features in the images. Shallow or poorly defined defects might be challenging for the current image processing pipeline to reliably detect and measure.

4. Discussion

The results of this study demonstrate the feasibility and potential of using a relatively simple image processing pipeline, guided by laser-generated reference points, for the automated measurement and detection of potential defects in welded samples. The high consistency observed in the measurement verification procedure (Section 3.1) underscores the reliability of the laser-assisted referencing system and the accuracy of the initial image calibration. This level of precision in establishing the pixel-to-millimeter scale is crucial for the subsequent dimensional analysis of weld features and potential defects.

The performance of the developed referenced measurement software (Section 3.2) indicates its capability to effectively integrate the laser-based calibration with image processing techniques for automated analysis. The software's ability to consistently detect the reference points across different weld surfaces highlights the robustness of the initial image processing steps involving color-based segmentation. This automated detection and calibration significantly reduces the need for manual intervention and the associated potential for human error, aligning with the broader goals of automated optical testing systems discussed in previous studies.

The comparison between the software-generated dimensional measurements and manual measurements (Section 3.3) reveals a promising level of accuracy, with average differences falling within a narrow range. This suggests that the developed image processing techniques, when calibrated using the laser reference, can provide quantitative data on the size of potential weld defects with reasonable precision. While direct comparison with irregularly shaped defects posed a challenge, the visual correlation with manual estimations supports the software's ability to identify and approximate the extent of these anomalies. This capability is particularly relevant when considering industry standards like EN ISO 5817, which often specify acceptance criteria based on the dimensions of weld imperfections. The developed system offers a potential tool for objectively assessing weld quality against such dimensional requirements.

The discussion of system robustness and limitations (Section 3.4) highlights important considerations for practical implementation. While the system showed some tolerance to variations in lighting and surface conditions, extreme cases of glare or poor defect visibility remain challenges. The estimated accuracy range is

influenced by the image resolution and the precision of the centroid detection, factors that could be further improved with higher-resolution imaging equipment and more sophisticated sub-pixel localization algorithms. The difficulty in detecting shallow or poorly defined defects points towards potential future research directions, possibly involving advanced image enhancement techniques or the integration of different imaging modalities.

Interpreting these results in the context of previous studies, our approach offers a potentially more costeffective and simpler alternative to some complex deep learning-based methods, particularly for applications where real-time performance and resource constraints are significant factors. While deep learning models (as discussed in the Introduction and exemplified by CU-Net in the initial example article) can offer superior robustness and feature learning capabilities, the developed laser-referenced image processing system provides a direct and interpretable method for dimensional measurement, which is a key requirement in many quality control scenarios. The integration of a physical reference directly onto the sample addresses the scale ambiguity inherent in single-view image analysis, a common challenge in TCV-based methods.

Future research directions could focus on enhancing the system's robustness to challenging lighting conditions and surface properties. Exploring advanced image preprocessing techniques, such as adaptive histogram equalization or specular reflection removal algorithms, could improve the reliability of defect detection and measurement. Investigating the integration of machine learning for automated defect classification based on the extracted dimensional and morphological features could further enhance the system's capabilities. Additionally, exploring the potential for real-time implementation by optimizing the image processing algorithms and leveraging more powerful embedded computing platforms would be a valuable next step towards industrial deployment.

These findings not only validate the technical feasibility of the proposed method but also suggest broader applicability in industrial quality control settings, particularly for automated visual inspection systems in welding processes. The integration of a low-cost, interpretable, and scalable measurement pipeline has the potential to reduce inspection time and human error while ensuring compliance with international welding standards. Future research could extend the system to multi-angle imaging or 3D reconstruction to capture complex weld geometries, and explore domain adaptation techniques to generalize the approach across different material types, welding methods, and industrial environments.

5. Conclusion

This study has presented a methodology for the automated determination of weld quality using an image

processing approach guided by laser-generated reference points. The developed system demonstrates the potential for accurate dimensional measurement of weld features and potential defects, offering a more objective and potentially faster alternative to traditional manual inspection methods. The measurement verification procedure confirmed the reliability of the laser-based calibration, and the referenced measurement software provided consistent results in identifying and measuring potential anomalies in welded samples. While the system exhibits certain limitations regarding challenging imaging conditions and the detection of subtle defects, the findings suggest that this approach holds promise for practical applications in weld quality control, particularly where cost-effectiveness and interpretability are key considerations. Future work will focus on enhancing the system's robustness, integrating machine learning for defect classification, and exploring its potential for realtime industrial implementation.

Author Contributions

The percentages of the authors' contributions are presented below. All authors reviewed and approved the final version of the manuscript.

	E.B.	E.G.
С	50	50
D	50	50
S	50	50
DCP	50	50
DAI	50	50
L	50	50
W	50	50
CR	50	50
SR	50	50
PM	50	50
FA	50	50

C=Concept, D= design, S= supervision, DCP= data collection and/or processing, DAI= data analysis and/or interpretation, L= literature search, W= writing, CR= critical review, SR= submission and revision, PM= project management, FA= funding acquisition.

Conflict of Interest

The authors declared that there is no conflict of interest.

References

Ajmi C, Zapata J, Elferchichi S, Laabidi K. 2024. Advanced fasterrcnn model for automated recognition and detection of weld defects on limited x-ray image dataset. J Nondestruct Eval, 43(1): 14.

Akkus A, Gorgun E. 2015. The investigation of mechanical behaviors of poly methyl methacrylate (PMMA) with the addition of bone ash, hydroxyapatite and keratin. Adv Mater, 4(1): 16-19.

Cardellicchio A, Nitti M, Patruno C, Mosca N, Di Summa M, Stella E, Renò V. 2024. Automatic quality control of aluminium parts

- welds based on 3D data and artificial intelligence. J Intell Manuf, 35(4): 1629–1648.
- Gook S, El-Sari B, Biegler M, Rethmeier M. 2024. Application of Al-based welding process monitoring for quality control in pipe production. Paton Weld J. 2024(6).
- Gorgun E. 2022. Characterization of superalloys by artificial neural network method. Int Symp Appl Math Eng (ISAME22), January 21-23, 2022, Istanbul, Türkiye, pp. 67.
- Gorgun E. 2024. Investigation of the effect of SMAW parameters on properties of AH36 joints and the chemical composition of seawater. Int J Innov Eng Appl, 8(1): 28–36.
- Gorgun E. 2024. Numerical analysis of inflow turbulence intensity impact on the stress and fatigue life of vertical axis hydrokinetic turbine. Phys Fluids, 36(1).
- Gorgun E, Karamis MB. 2019. Ultrasonic testing to measure the stress statement of steel parts. J Mech Sci Technol, 33(7): 3231–3236.
- Guo Q, Yang Z, Xu J, Jiang Y, Wang W, Liu Z, Zhao W, Sun Y. 2024. Progress, challenges and trends on vision sensing technologies in automatic/intelligent robotic welding: Stateof-the-art review. Robot Comput Integr Manuf, 89: 102767.
- Islam MR, Zamil MZH, Rayed ME, Kabir MM, Mridha MF, Nishimura S, Shin. 2024. Deep learning and computer vision techniques for enhanced quality control. IEEE Access, Manuf Process, Seoul, South Korea, pp:52-60.
- Ji W, Luo Z, Luo K, Shi X, Li P, Yu Z. 2024. Computer vision-based surface defect identification method for weld images. Mater Lett, 371: 136972.
- Liu W, Hu J, Qi J. 2025. Resistance spot welding defect detection based on visual inspection. Improved Faster R-CNN model. Machines. 13(1): 33.
- Lopez-Fuster MA, Morgado-Estevez A, Diaz-Cano I, Badesa FJ. 2024. A neural-network-based cost-effective method for initial weld point extraction from 2D images. Machines, 12(7): 447.
- Mobaraki M. 2025. Vision-based seam tracking and multi-modal defect detection in GMAW fillet welding using artificial intelligence. PhD Thesis, University of British Columbia, pp:

- 45-49
- Pham DA, Bui DQ, Le TD, Tran DH, Nguyen TH. 2024. Automatic welding seam tracking and real-world coordinates identification with machine learning method. Results Eng, 23: 102565
- Stavropoulos P, Sabatakakis K. 2024. Quality assurance in resistance spot welding: state of practice, state of the art, and prospects. Metals, 14(2): 185.
- Sutherland C, Henderson AD, Giosio DR, Trotter AJ, Smith GG. 2024. Synchronising an IMX219 image sensor and AS7265x spectral sensor to make a novel low-cost spectral camera. HardwareX. 19: e00573.
- Voelkel J, Meissner M, Bartsch H, Feldmann M. 2024. The influence of external weld imperfection size on the load-bearing capacity of butt-welded joints. J Constr Steel Res, 220: 108808
- Wang Y, Lee W, Jang S, Truong VD, Jeong Y, Won C, Lee J, Yoon J. 2024. Prediction of internal welding penetration based on IR thermal image supported by machine vision and ANN-model during automatic robot welding process. J Adv Join Process, 9: 100199.
- Xu J, Hu X, Zhan H. 2025. CU-NET: Context extractor network based U-Net for magnetic tile segmentation. In: Proc Int Conf Equip Intell Oper Maint (ICEIOM 2023), Hefei, China, Sep 21– 23, 2023 (Vol II). CRC Press: 155.
- Yu Q, Xiao L, Zheng D, Peng Z, Song K. 2024. A computer vision-based lithium battery tab welding quality detection system. Trans China Weld Inst, 45(10): 38–49.
- Yue Y. 2024. Research on welding seam detection and recognition technology for industrial boilers. Proc 2024 IEEE 7th Inf Technol Netw Electron Autom Control Conf (ITNEC): IEEE: 413–416.
- Zhang B, Wang X, Cui J, Wu J, Xiong Z, Zhang W, Yu X. 2024. Enhancing weld inspection through comparative analysis of traditional algorithms and deep learning approaches. J Nondestruct Eval, 43(2): 38.